Synthesis and Properties of Multi-Triarylamine-Substituted Carbazole-Based Dendrimers with an Oligothiophene Core for Potential Applications in Organic Solar Cells and Light-Emitting Diodes

Jianping Lu,[†] Ping Fang Xia,[‡] Pik Kwan Lo,[‡] Ye Tao,*[,†] and Man Shing Wong*[,‡]

Institute for Microstructural Sciences (IMS), National Research Council of Canada (NRC), 1200 Montreal Road, Ottawa, Ontario K1A 0R6, Canada, and Department of Chemistry and Centre for Advanced Luminescence Materials, Hong Kong Baptist University, Kowloon Tong, Hong Kong SAR, China

Received September 5, 2006. Revised Manuscript Received October 19, 2006

In this paper, we report on the synthesis and properties of a novel series of multi-triarylamine-substituted carbazole-based dendrimers G_2-OTP(n)-G_2 ($n = 2-5$) with an oligothiophene core. The length of the oligothiophene core varied from 2 to 5 thiophene units. It was found that both the absorption and fluorescence emission peaks red-shifted with increasing oligothiophene core length. As a result, the power conversion efficiencies of the as-fabricated solar cells using the composite of these dendrimers and PCBM as the photoactive layer increased with increasing oligothiophene core length, from 0.04% for G_2-DTP-G_2 to 0.13% for G_2-PTP-G_2 under AM 1.5 simulated solar illumination at an irradiation intensity of 100 mW/cm^2. After a thermal annealing at 150 °C for 15 min under nitrogen, however, the devices based on the G_2-DTP-G_2:PCBM blend exhibited the most dramatic improvement and almost best performance, although other devices also showed some improvement. Since only G_2-DTP-G_2 is the a crystalline material among these four dendrimers, the dramatic improvement of the associated devices after annealing is attributed to the formation of some nanocrystalline structures in the active layer, as indicated by DSC analysis and AFM studies. In addition, we have demonstrated that both G_2-DTP-G_2 and G_2-PTP-G_2 can be used as hole-transporting emitters in organic light-emitting diodes (OLEDs) with 1,3,5-tris(*N*-phenylbenzimidazol-2-yl)benzene (TPBI) as a hole-blocking layer and LiF/Al as the cathode. Because of the low hole injection barrier, the turn-on voltages of the OLED devices were as low as 4 V. G_2-DTP-G_2 exhibited blue electroluminescence with a maximum luminance of 1660 cd/m^2 at 15.5 V, while G_2-PTP-G_2 emitted yellow light with a highest luminance of 1000 cd/m^2 at 19 V.

Introduction

Conversion of sunlight directly into electricity via photovoltaic (PV) devices is being recognized as an essential part of future global energy production.[1] The demand for inexpensive and renewable energy sources is the driving force for the development of high-efficiency low-cost PV devices. Since the discovery of efficient photoinduced charge separation at donor−acceptor interfaces,[2] organic solar cells based on conjugated polymers and soluble fullerenes have been intensively studied.[3−6] This "bulk heterojunction" strategy is widely used due to its simple device structure, easy thin-film casting process, low fabrication cost, and high power conversion efficiency (PCE). Due to the short exciton diffusion length of most conjugated polymers (approximately 10 nm), electron donor and acceptor materials have to be blended forming bicontinuous phase-separated structures with the size of each phase comparable to the exciton diffusion length to achieve high efficiencies. Recent advances in the control of the nanostructured morphology of the interpenetrating donor/acceptor networks boosted the efficiencies to the 5% range by postproduction thermal annealing,[7−9] active layer electric aging,[7] and solidification time controlling.[10]

Dendritic macromolecules provide unique molecular architectures for a wide variety of applications in optoelectronic and electronic devices.[11−15] They can be designed to possess

* To whom all correspondence should be addressed: Phone: (613) 998-2485. Fax: (613) 990-0202. E-mail: Ye.Tao@nrc-cnrc.ca (Y.T.); mswong@hkbu.edu.hk (M.S.W.).

[†] National Research Council of Canada.

[‡] Hong Kong Baptist University.

(1) Shaheen, S. E.; Ginley, D. S.; Jabour, G. E. *MRS Bull.* **2005**, *30*, 10.
(2) Sariciftci, N. S.; Smilowitz, L.; Heeger, A. J.; Wudl, F. *Science* **1992**, *258*, 1474.
(3) Yu, G.; Gao, J.; Hummelen, C. J.; Wudl, F.; Heeger, A. J. *Science* **1995**, *270*, 1789.
(4) Brabec, C. J.; Sariciftci, N. S.; Hummelen, J. C. *Adv. Funct. Mater.* **2001**, *11*, 15.
(5) Hoppe, H.; Sariciftci, N. S. *J. Mater. Chem.* **2006**, *16*, 45.
(6) Krebs, F.; Spanggaard, H. *Chem. Mater.* **2005**, *17*, 5235.
(7) Padinger, F.; Rittberger, R. S.; Sariciftci, N. S. *Adv. Funct. Mater.* **2003**, *13*, 85.
(8) Kim, Y.; Choulis, S. A.; Nelson, J.; Bradley, D. D. C.; Cook, S.; Durrant, J. R. *Appl. Phys. Lett.* **2005**, *86*, 63502.
(9) Ma, W.; Yang, C.; Gong, X.; Lee, K.; Heeger, A. J. *Adv. Funct. Mater.* **2005**, *15*, 1617.
(10) Li, G.; Shrotriya, V.; Huang, J.; Yao, Y.; Moriarty, T.; Emery, K.; Yang, Y. *Nat. Mater.* **2005**, *4*, 826.
(11) Pogantsch, A.; Wenzl, F. P.; List, E. J. W.; Leising, G.; Grimsdale, A. C.; Müllen, K. *Adv. Mater.* **2002**, *14*, 1061.
(12) Ma, D.; Lupton, J. M.; Samuel, I. D. W.; Lo, S.-C.; Burn, P. L. *Appl. Phys. Lett.* **2002**, *81*, 2285−2287.
(13) Furuta, P.; Brooks, J.; Thompson, M. E.; Fréchet, J. M. J. *J. Am. Chem. Soc.* **2003**, *125*, 13165−13172.
(14) Kwon, T. W.; Alam, M. M.; Jenekhe, S. A. *Chem. Mater.* **2004**, *16*, 4657.

10.1021/cm062111o CCC: $33.50
Published on Web 12/19/2006

conjugated cores for an efficient emission and/or charge transport and appropriate terminal groups/chains for good processibility. To the best of our knowledge, however, there are only a few reports on the applications of dendrimers in organic solar cells.[16−18]

In this study, a novel series of multi-triarylamine-substituted carbazole-based dendrimers G_2-OTP(n)-G_2 (n = 2−5) bearing an oligothiophene as a functional core were designed and synthesized. The length of the oligothiophene core varied from thiophene dimer to pentamer. The photophysical and electrochemical properties of the resulting dendrimers and their performance as light-absorbing and hole transporting components in organic solar cells were systematically investigated. It was found that both the absorption and photoluminescence (PL) emission peaks red-shifted with increasing oligothiophene core length, leading to a better match with the solar spectrum. As a result, under AM 1.5 simulated solar illumination at an irradiation intensity of 100 mW/cm^2, the power conversion efficiencies of the as-fabricated solar cells using the composite of these dendrimers and PCBM (methanofullerene [6,6]-phenyl C_{61}-butyric acid methyl ester) as a photoactive layer increased with an increase in the oligothiophene conjugation length. After a thermal annealing at 150 °C for 15 min under nitrogen, however, the devices based on the G_2-DTP-G_2:PCBM blend (containing only 2 thiophene units) exhibited the most dramatic improvement and almost best performance with J_{sc} = 1.08 mA/cm^2, V_{oc} = 0.85 V, FF = 0.31, although other devices also showed some mild improvement. Since the UV−vis absorption spectra showed negligible changes for all G_2-OTP(n)-G_2:PCBM based devices after the annealing, the enhanced photocurrent generation was most likely caused by the improvement in charge carrier mobility and/or charge separation. Considering the fact that G_2-DTP-G_2 has the lowest absorption in the solar spectrum among these four dendrimers and is the only one showing a melting peak in the DSC analysis, we speculate that the dramatic improvement in the device performance of G_2-DTP-G_2 after annealing is attributed to the formation of ordered structures in the active layer. DSC analysis confirmed the formation of a semicrystalline phase in the G_2-DTP-G_2 sample, which had undergone a DSC scan, followed by a thermal annealing at 150 °C for 15 min.

Although the fluorescence (FL) efficiencies of polythiophenes and oligothiophenes in the solid state are usually low due to the increased contribution of nonradiative decay via interchain interactions and intersystem crossing caused by the heavy-atom effect of sulfur,[19,20] G_2-DTP-G_2 (18%) and G_2-PTP-G_2 (7%) have moderate solid-state FL efficiency. This is probably due to the presence of bulky wedges at the end of the oligothiophenes, which can diminish the interchain interaction. Furthermore, we demonstrated in this paper that both G_2-DTP-G_2 and G_2-PTP-G_2 could be used as hole-transporting emitters in organic light-emitting diodes (OLEDs) with TPBI as a hole-blocking layer and LiF/Al as the cathode. Because of the low hole injection barrier, the turn-on voltages of the fabricated OLED devices were as low as 4 V. The neat G_2-DTP-G_2 film-based blue light-emitting diodes showed a maximum luminance of 1660 cd/m^2 at 15.5 V, while G_2-PTP-G_2 emitted yellow light with a highest luminance of 1000 cd/m^2 at 19 V.

Experimental Section

Materials. Reagent grade solvents and chemicals were used as received unless otherwise noted. Poly(3,4-ethylenedioxythiophene)−poly(styrene sulfonate) (PEDOT−PSS) in aqueous solution and methanofullerene [6,6]-phenyl C_{61}-butyric acid methyl ester (PCBM) were purchased from Bayer corporation and American Dye Source Inc., respectively. The synthetic route for the preparation of carbazole-based oligothiophene dendrimer, G_2-OTP(n)-G_2, is summarized in Scheme 1. The synthetic procedures for 3,6-bis[4-(diphenylamino)-1-phenyl]carbazole (G_2-H),[21] 5,5′-diiodo-2,2′-bithiophene,[22] and 5,5″-diiodo-2,2′:5′,2″-terthiophene[22] were reported previously.

Characterization. ^{1}H and ^{13}C NMR spectra were obtained in $CDCl_3$ on a 400 MHz Varian Unity Inova spectrometer. High-resolution mass spectrometric measurements were carried out using a Bruker autoflex MALDI-TOF mass spectrometer. UV−vis absorption spectra were recorded on a Varian Cary 50 spectrophotometer. Fluorescence measurements were carried out on a Spex Fluorolog 3 spectrometer. The differential scanning calorimetry (DSC) analysis of dendrimers was performed under a nitrogen atmosphere on a TA Instruments DSC 2920 at heating rates of 10 °C/min. Cyclic voltammetry (CV) measurements were conducted in a 0.1 M Bu_4NPF_6 acetonitrile solution using a Solartron SI 1287 potentiostat at a scan rate of 100 mV s^{-1} at room temperature under argon. A silver wire (2 mm diameter), a platinum wire (0.5 mm diameter), and a platinum disk (1 mm diameter) sealed in a soft glass rod were used as the quasireference electrode, counter electrode, and working electrode, respectively. The Ag quasi-reference electrode was calibrated using a ferrocene/ferrocenium redox couple as an external standard prior to measurements.

PV Device Fabrication and Testing. ITO-coated glass substrates (15 Ω/□) were patterned by a conventional wet-etching process using an acid mixture of HCl (6 N) and HNO_3 (0.6 N) as the etchant. The active area of each solar cell device was 5 × 5 mm^2. After patterning, the substrates were rinsed in deionized water, and then ultrasonicated sequentially in acetone (20 °C) and 2-propanol (65 °C). Immediately prior to device fabrication, the ITO substrate was treated in a UV−ozone oven for 15 min. Subsequently, a poly(3,4-ethylenedioxythiophene)−poly(styrene sulfonate) (PEDOT−PSS) thin film (50 nm) was spin-coated at 5000 rpm from its aqueous solution onto the treated substrate, and then baked at 140 °C under nitrogen for 30 min. The active layer composed of the blend of G_2-OTP(n)-G_2 and PCBM at various ratios was then spin-coated on top of PEDOT−PSS from chlorobenzene solutions at 800 rpm for 60 s. The thickness of the resulting film was found to be about 110 nm, as measured with a Dektak III surface pro-

(15) Ponomarenko, S. A.; Kirchmeyer, S.; Elschner, A. *Adv. Funct. Mater.* **2003**, *13*, 591.
(16) Satoh, N.; Nakashima, T.; Yamamoto, K. *J. Am. Chem. Soc.* **2005**, *127*, 13030−13038.
(17) Hasobe, T.; Kashiwagi, Y.; Absalom, M. A.; Sly, J.; Hosomizu, K.; Crossley, M. J.; Imahori, H.; Kamat, P. V.; Fukuzumi, S. *Adv. Mater.* **2004**, *16*, 975−979, 946.
(18) Bettignies, R.; Nicolas, Y.; Blanchard, P.; Levillain, E.; Nunzi, J.-M.; Roncali, J. *Adv. Mater,* **2003**, *15*, 1939.
(19) Chen, F.; Mehta, P. G.; Takiff, L.; McCullough, R. D. *J. Mater. Chem.* **1996**, *6*, 1763.
(20) Perepichka, I. F.; Perepichka, D. F.; Meng, H.; Wudl, F. *Adv. Mater.* **2005**, *17*, 2281.
(21) Li, H. Z.; Wong, M. S. *Org. Lett.* **2006**, *8*, 1499.
(22) Li, Z. H.; Wong, M. S.; Tao, Y.; Fukutani, H. *Chem. Mater.* **2005**, *17*, 5032.

Scheme 1. Synthetic Route to Multi-Triarylamine-Substituted Carbazole-Based Dendrimers G_2-OTP(n)-G_2, $n = 2-5$

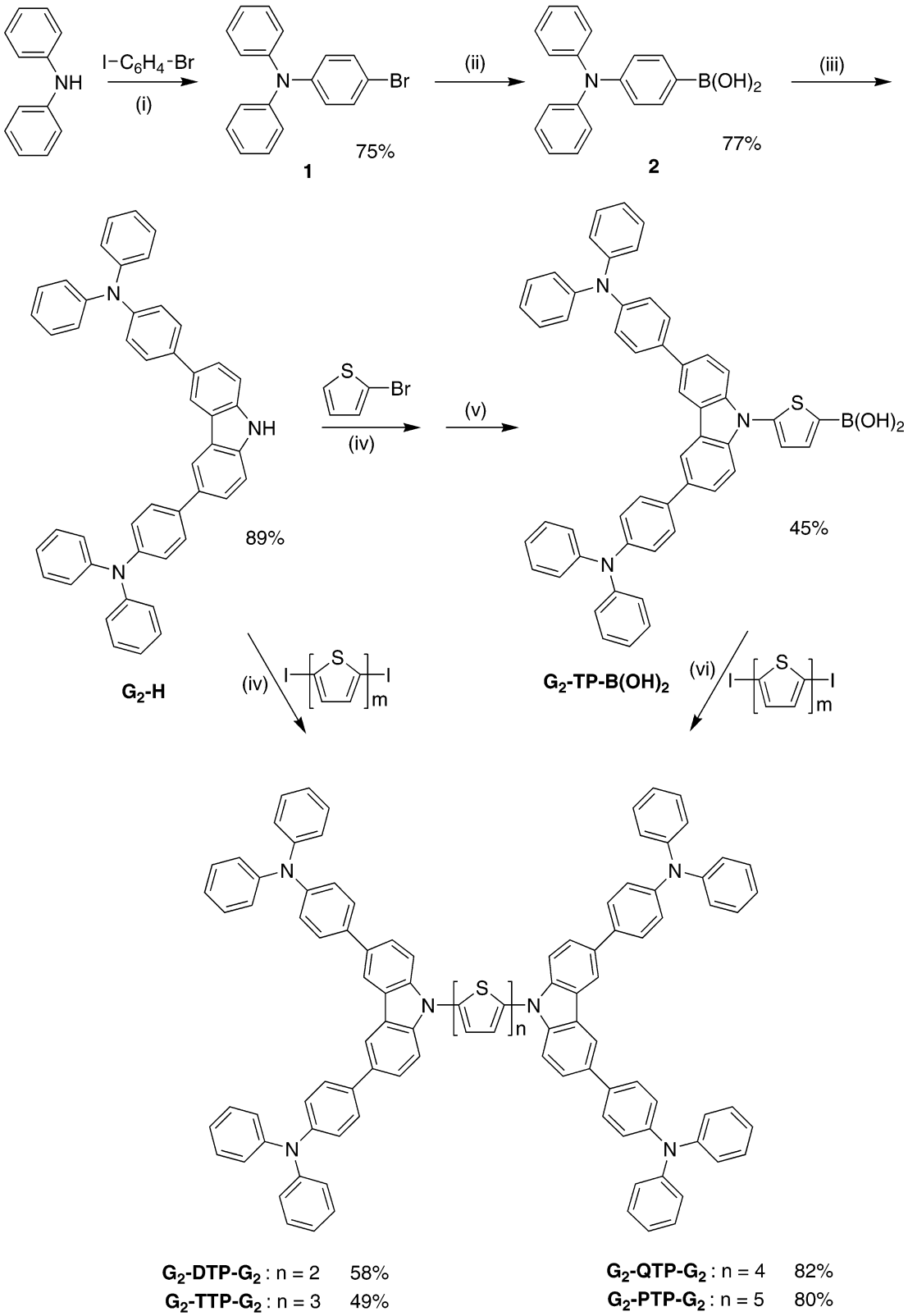

(i) 1 mole% CuI, 10 mole% 1,2-trans-cyclohexadiamine, NaO*t*Bu, dioxane, 110 °C; (ii) a 1.5 equiv. *n*-BuLi, THF, −78 °C; b $B(OCH_3)_3$, −78 °C to r.t.; c 6M HCl; (iii) 3,6-dibromocarbazole, 2.5 mole% $Pd(PPh_3)_4$, THF, 2M K_2CO_3, 80 °C; (iv) 25 mole% CuI, 250 mole% 1,2-*trans*-cyclohexadiamine, NaO*t*Bu, dioxane, 110 °C; (v) a 4 equiv. *n*-BuLi, THF, −20 °C to r.t; b $B(OCH_3)_3$, 0 °C to r.t.; c 2M HCl; (vi) 5 mole% $Pd(PPh_3)_4$, 2M K_2CO_3, THF, 80 °C.

filometer. The device fabrication was completed by the vacuum deposition of LiF (1 nm) and Al cathode (100 nm). Postproduction device annealing was carried out at 150 °C for 15 min under nitrogen. The solar cells with no protective encapsulation were subsequently tested in air under air mass (AM) 1.5 simulated solar illumination (100 mW/cm^2, Sciencetech Inc., model SF150). Current−voltage ($I-V$) characteristics were recorded using a computer-controlled Keithley 2400 source meter.

EL Device Fabrication and Testing. ITO-coated glass substrates (15 Ω/□) were patterned and cleaned using the same procedure as

that used for the PV devices. Immediately before device fabrication, the ITO substrate was UV−ozone treated for 15 min. Subsequently, PEDOT−PSS (50 nm) was spin-coated at 5000 rpm from its aqueous solution onto the treated substrate, and then baked at 140 °C under nitrogen for 30 min. G_2-DTP-G_2 or G_2-PTP-G_2 was dissolved in a solvent mixture of $CHCl_3$ and chlorobenzene (1:1 by volume), and then spin-coated on PEDOT−PSS. TPBI was vacuum-deposited as a hole-blocking layer. Finally, LiF (1 nm) and Al (100 nm) were deposited as the cathode. The devices were tested in air under ambient conditions with no protective encapsulation. EL spectra, device luminances, and current−voltage characteristics were recorded using a combination of a Photo Research PR-650 SpectraScan and a Keithley 238 Source meter.

5,5′-Bis{3,6-bis[4-(diphenylamino)-1-phenyl]carbazol-9-yl}-2,2′-bithiophen e (G_2-DTP-G_2). A mixture of G_2H (654 mg 1.00 mmol), 5,5′-diiodo-2, 2′,bithiophene (209 mg, 0.50 mmol), (±)-*trans*-1,2-diaminocyclohexane (285 mg, 2.5 mmol), CuI (47 mg. 0.25 mmol), sodium *tert*-butoxide (250 mg, 2.6 mmol), and dioxane (30 mL) was heated at 110 °C for 45 h under nitrogen atmosphere. After cooling to room temperature, the reaction mixture was poured into cooled water and extracted with CH_2Cl_2 (3 × 50 mL). The crude product was purified by silica-gel column chromatography using 4:1 petroleum ether/CH_2Cl_2 as eluent affording 428 mg (58%) of a pale yellow solid. ^{1}H NMR (400 MHz, $CDCl_3$, δ) 8.30 (d, J = 1.2 Hz, 4H, carbazole-H), 7.68 (dd, J = 1.6, 8.8 Hz, 4H, Ar−H), 7.59 (m, 12H, Ar−H), 7.23−7.30 (m, 16H, Ar−H), 7.12−7.19 (m, 28H, Ar−H and TP−H), 7.01 (t, J = 7.6 Hz, 8H, p-Ph_2N−H). ^{13}C NMR (100 MHz, $CDCl_3$, δ) 147.8, 146.7, 141.3, 137.7, 135.8, 135.2, 134.1, 129.3, 128.0, 125.7, 125.4, 124.3, 124.2, 122.8, 122.7, 118.3, 110.6. MS (FAB) m/z 1469.9 (M^+). HRMS (MALDI-TOF) Calcd for $C_{104}H_{72}N_6S_2$: 1469.5291 (M^+). Found: 1469.5243.

5,5″-Bis{3,6-bis[4-(diphenylamino)-1-phenyl]carbazol-9-yl}-2,2′:5′,2″-terthi ophene (G_2-TTP-G_2). A mixture of G_2H (987 mg 1.51 mmol), 5,5″-diiodo-2,2′:5′,2″-terthiophene (377 mg, 0.75 mmol), (±)-*trans*-1,2-diaminocyclohexane (430 mg, 3.77 mmol), CuI (72 mg. 0.38 mmol), sodium *tert*-butoxide (377 mg, 3.93 mmol), and dioxane (40 mL) was heated at 110 °C for 60 h under nitrogen atmosphere. After cooling down to room temperature, the reaction mixture was poured into cooled water and extracted with CH_2Cl_2 (3 × 60 mL). The crude product was purified by silica-gel column chromatography using 4:1 petroleum ether/CH_2Cl_2 as eluent affording 570 mg (49%) of a yellow solid. ^{1}H NMR (400 MHz, $CDCl_3$, δ) 8.30 (d, J = 0.8 Hz, 4H, carbazole-H), 7.62 (dd, J = 1.2, 8.8 Hz, 4H, Ar−H), 7.55 (m, 12H, Ar−H), 7.22−7.26 (m, 16H, Ar−H), 7.12−7.17 (m, 26H, Ar−H and TP−H), 7.05−7.07 (m, 4H, TP−H), 7.00 (t, J = 7.6 Hz, 8H, p-Ph_2N−H). ^{13}C NMR (100 MHz, $CDCl_3$, δ) 147.7, 146.6, 141.2, 137.4, 136.1, 135.7, 135.0, 134.0, 129.2, 127.9, 125.6, 125.2, 124.6, 124.3, 124.2, 122.7, 122.4, 118.3, 110.6. HRMS (MALDI-TOF) Calcd for $C_{108}H_{74}N_6S_3$: 1551.5168. Found: 1551.5101.

2-{3,6-Bis[4-(diphenylamino)-1-phenyl]carbazol-9-yl}-thiophene (G_2-TP). A mixture of G_2-H (840 mg, 1.28 mmol), 2-bromothiophene (417 mg, 2.56 mmol) copper iodide (60 mg, 0.32 mmol), (±)-*trans*-1,2-diaminocyclohexane (365 mg, 3.20 mmol), sodium *tert*-butoxide (320 mg, 3.33mmol), and dioxane (40 mL) was heated under nitrogen atmosphere at 110 °C with good stirring for 40 h. After cooling to room temperature, the reaction mixture was poured into cooled water and extracted with $CHCl_3$ (5 × 60 mL). The combined organic layer was dried with anhydrous Na_2SO_4 and evaporated to dryness. The crude product was purified by silica-gel column chromatography using petroleum ether/$CHCl_3$ as gradient eluent. The target compound was obtained as a white solid with an isolated yield of 74% (696 mg). ^{1}H NMR (400 MHz, $CDCl_3$, δ) 8.32 (d, J = 1.6 Hz, 2 H, carbazole-H), 7.67 (dd, J = 1.6, 8.8 Hz, 2H, Ar−H), 7.60 (d, J = 8.8 Hz, 4H, Ar−H), 7.51 (d, J = 8.8 Hz, 2H, Ar−H), 7.41 (dd, J = 1.6, 5.6 Hz, 1H, TP−H), 7.22−7.30 (m, 8H, Ar−H), 7.15−7.21 (m, 14H, Ar−H and TP−H), 7.03 (t, J = 7.6 Hz, 4H, p-Ph_2N−H). ^{13}C NMR (100 MHz, $CDCl_3$, δ) 147.8, 146.6, 141.6, 136.0, 133.8, 129.2, 127.9, 126.3, 125.5, 124.6, 124.3, 124.2, 124.15, 124.1, 122.7, 118.3, 110.5. HRMS (MALDI-TOF) Calcd for $C_{52}H_{37}N_3S$ 735.2708. Found: 735.2715.

5-{3,6-Bis[4-(diphenylamino)-1-phenyl]carbazol-9-yl}-2-thiopheneboronic Acid (G_2-TP-B$(OH)_2$). To a 100 mL two-necked flask containing the solution of G_2TP (368 mg, 0.5 mmol) in 40 mL dried THF equipped with a magnetic stirrer under N_2 atmosphere at −20 °C was added dropwise 1.6 M *n*-BuLi (1.25 mL, 2.0 mmol) while maintaining good stirring. After the reaction mixture was stirred for 15 min at −20 °C followed by 1 h at room temperature, trimethylborate (0.25 mL, 2.2 mmol) was added at 0 °C. The reaction mixture was then allowed to warm up to room temperature. After 5 h of stirring at room temperature, water was added to the reaction, followed by acidifying with 2 M HCl. The solution mixture was extracted with CH_2Cl_2 (3 × 50 mL). The combined organic layer was dried with anhydrous Na_2SO_4, filtered, and evaporated to dryness. The crude product was purified by silica-gel flash column chromatography using CH_2Cl_2/EtOAc (v/v = 3:1) as eluent affording a deep-brown solid with an isolated yield of 45% (176 mg). ^{1}H NMR (400 MHz, DMSO-d_6, δ) 8.65 (d, J = 1.2 Hz, 2H, carbazole-H), 8.51 (s, 2H, B$(OH)_2$-H), 7.83 (d, J = 4 Hz, 1H, TP−H), 7.78 (dd, J = 1.6, 8.4 Hz, 2H, Ar−H), 7.74 (d, J = 8.4 Hz, 4H, Ar−H), 7.58 (d, J = 8.8 Hz, 2H, Ar−H), 7.46 (d, J = 4 Hz, 1H, TP−H), 7.30−7.34 (m, 8H, Ar−H), 7.03−7.11 (m, 16H, Ar−H). ^{13}C NMR (100 MHz, $CDCl_3$, δ) 147.2, 146.2, 142.5, 140.3, 135.7, 135.0, 132.9, 129.6, 127.8, 125.3, 125.2, 124.0, 123.9, 123.0, 118.5, 110.6.

5,5‴-Bis{3,6-bis[4-(diphenylamino)-1-phenyl]carbazol-9-yl}-2,2′:5′,2″:5″,2‴-quaterthiophene (G_2-QTP-G_2). To a mixture of G_2-TP-B$(OH)_2$ (260 mg, 0.33 mmol), 5,5′-diiodo-2,2′-bithiophene (67 mg, 0.16 mmol), and tetrakis(triphenylphosphine)-palladium(0) (38 mg, 0.33 mmol) in a 100 mL-round-bottom flask equipped with a magnetic stirrer, a N_2 purge, and a reflux condenser was added THF (30 mL) and 2 M K_2CO_3 (2 mL). The solution mixture was heated to 80 °C for overnight. The reaction mixture was poured into water and then extracted with chloroform (5 × 50 mL). The combined organic layer was dried with anhydrous Na_2SO_4, filtered, and evaporated to dryness. The crude product was purified by silica-gel column chromatography using petroleum ether/$CHCl_3$ and $CHCl_3$/EtOAc as eluent affording 214 mg (82%) of an orange solid. ^{1}H NMR (400 MHz, $CDCl_3$, δ) 8.30 (d, J = 1.6 Hz, 4H, carbazole-H), 7.64 (dd, J = 1.6, 8.8 Hz, 4H, Ar−H), 7.54−7.58 (m, 12H, Ar−H), 7.22−7.27 (m, 16H, Ar−H), 7.13−7.18 (m, 26H, Ar−H and TP−H), 7.10 (d, J = 4 Hz, 2H, TP−H), 7.08 (s, 4H, TP−H), 7.01 (t, J = 7.6 Hz, 8H, p-Ph_2N−H). ^{13}C NMR (100 MHz, $CDCl_3$, δ) 147.7, 146.7, 141.2, 137.3, 136.1, 135.9, 135.8, 135.1, 134.0, 129.2, 129.0, 127.9, 125.6, 125.3, 124.7, 124.5, 124.3, 124.2, 122.8, 122.4, 118.3, 110.6. HRMS (MALDI-TOF) Calcd for $C_{112}H_{76}N_6S_4$: 1633.5046. Found: 1633.5017.

5,5⁗-Bis{3,6-bis[4-(diphenylamino)-1-phenyl]carbazol-9-yl}-2,2′:5′,2″:5″,2 ‴:5‴, 2⁗-quinquethiophene (G_2-PTP-G_2). The procedure above was followed using 228 mg (0.29 mmol) of G_2-TP-B$(OH)_2$, 72 mg (0.144 mmol) of 5,5″-diiodo-2,2′:5′,2″-terthiophene, 35 mg (0.03 mmol) of tetrakis(triphenylphosphine)-palladium(0), THF (30 mL), and 2 M K_2CO_3 (2 mL). The crude product was purified by column chromatography using petroleum ether/CH_2Cl_2 as a gradient eluent affording 197 mg (80%) of an orange-red solid. ^{1}H NMR (400 MHz, $CDCl_3$, δ) 8.30 (s, 4 H, carbazole-H), 7.65 (dd, J = 1.2, 8.4 Hz, 4H, Ar−H), 7.55−7.58

(m, 12H, Ar−H), 7.24−7.28 (m, 16H, Ar−H), 7.14−7.19 (m, 26H, Ar−H and TP−H), 7.06−7.11 (m, 8H, TP−H), 7.02 (t, J = 7.6 Hz, 8H, *p*-Ph_2N−H). ^{13}C NMR (100 MHz, $CDCl_3$, δ) 147.7, 146.7, 141.2, 137.3, 136.2, 135.9, 135.84, 135.77, 135.2, 134.0, 129.2, 127.9, 125.6, 125.3, 124.7, 124.5, 124.4, 124.3, 124.2, 122.8, 122.4, 118.3, 110.6. HRMS (MALDI-TOF) Calcd for $C_{116}H_{78}N_6S_5$: 1715.4923. Found: 1715.4920.

Results and Discussion

Synthesis. The synthetic route for the preparation of carbazole-based oligothiophene dendrimer, G_2-OTP(n)-G_2, is summarized in Scheme 1, which was synthesized by a convergent approach. Selective monoamination of 1-bromo-4-iodobenzene with diphenylamine catalyzed by CuI in the presence of sodium *t*-butoxide afforded 4-bromo-4′-(diphenylamino)biphenyl, **1** in 75% yield. Conversion of **1** to the corresponding boronic acid, **2**, was achieved by lithium-bromide exchange of **1** at −78 °C followed by the reaction with trimethyl borate and subsequent acid hydrolysis. Double Suzuki cross-coupling of boronic acid **2** and 3,6-dibromocarbazole afforded G_2-H in an excellent yield under typical reaction conditions. Double Ullmann−Goldberg coupling of G_2-H and diiodobithiophene and diiodoterthiophene afforded carbazole-based oligothiophene dendrimer G_2-DTP-G_2 and G_2-TTP-G_2, respectively, in moderate yields. The extended diiodo-oligothiophenes are highly insoluble and nontrivial to prepare with good purity; therefore, the synthesis of the higher homologues of oligothiophene dendrimers adopted an alternative approach, as shown in Scheme 1. Ullmann−Goldberg coupling of G_2-H and 2-bromothiophene gave carbazole-dendron substituted thiophene G_2-TP in good yield. Lithiation of G_2-TP at −20 °C followed by quenching with trimethyl borate and subsequent acid hydrolysis afforded the corresponding boronic acid, G_2-TP-$B(OH)_2$. Double Suzuki cross-coupling of G_2-TP-$B(OH)_2$ and diiodobithiophene and diiodoterthiophene afforded carbazole-based oligothiophene dendrimer G_2-QTP-G_2 and G_2-PTP-G_2, respectively, in 80−82% yield.

Thermal and Optical Properties of Dendrimers G_2-OTP(n)-G_2. Thermogravimetric analysis of four dendrimers G_2-OTP(n)-G_2 showed that they are all thermally stable with onset decomposition temperatures above 540 °C under nitrogen. DSC analysis revealed that these four dendrimers have similar glass transition temperatures (T_g's) ranging from 167 to 172 °C, although they have different oligothiophene cores. It is interesting to point out that only G_2-DTP-G_2 among these four dendrimers exhibited a melting peak (centered at 259.4 °C) during DSC analysis. The other three dendrimers are amorphous molecular materials and only show glass transition temperatures. However, even G_2-DTP-G_2 is not prone to crystallize, and no pronounced crystallization peak was observed in the DSC cooling scan. After the first DSC analytical scan, the G_2-DTP-G_2 sample was fast cooled to room temperature and then annealed at 150 °C for 15 min under N_2. The subsequent DSC scan showed a T_g at 169.6 °C and a broad melting peak appearing around 210−244 °C, as shown in Figure 1. This result indicates that a thermal annealing at 150 °C can lead to the formation of semicrystalline structures in G_2-DTP-G_2. The phenomenon

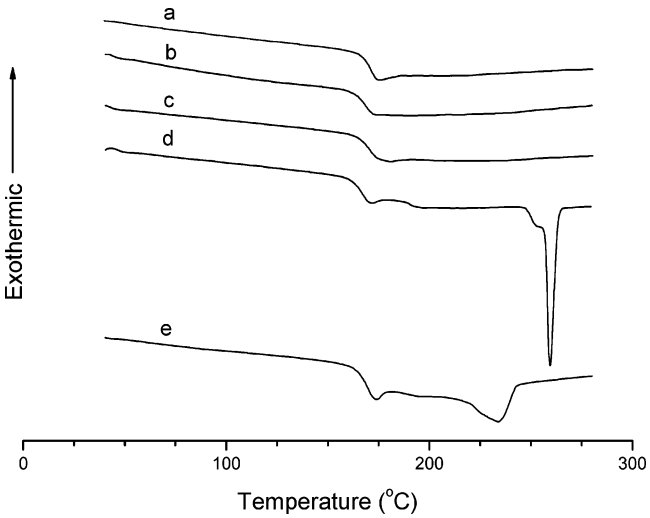

Figure 1. DSC thermograms of G_2-OTP(n)-G_2, (a) G_2-PTP-G_2, (b) G_2-QTP-G_2, (c) G_2-TTP-G_2, (d) G_2-DTP-G_2, and (e) G_2-DTP-G_2 annealed at 150 °C for 15 min after the first DSC scan.

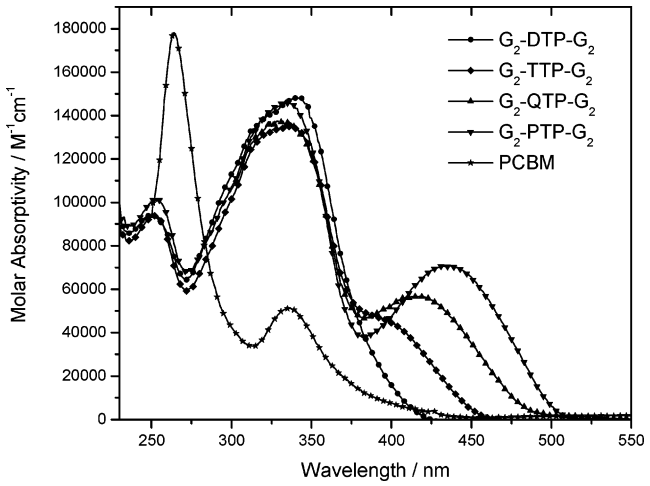

Figure 2. UV−vis absorption spectra of G_2-OTP(n)-G_2 and PCBM in chloroform.

that melting peaks become broader and shift to lower temperature when semicrystalline structures rather than perfect crystals are formed has been reported in the literature.[23,24]

The UV−vis absorption and PL spectra of G_2-OTP(n)-G_2 in chloroform are shown in Figures 2 and 3, respectively. For comparison purposes, the absorption spectrum of PCBM is also included in Figure 2. It is clear that G_2-OTP(n)-G_2 have stronger absorbance in the solar spectrum than PCBM. G_2-OTP(n)-G_2 shows two overlapped absorption bands peaked around 330 and 370−430 nm, which correspond to the n→π* transition of triarylamine-subtituted carbazole wedge[21] and π→π* transition of oligothiophene core, respectively. These two spectra indicate that both absorption and PL emission peaks of the oligothiophene core are gradually red-shifted to longer wavelengths with an increase in the number of thiophene units due to the increased effective conjugation length; however, the absorption of dendritic wedge remains fairly constant throughout the series.

(23) Dobbertin, J.; Hannemann, J.; Schick, C.; Pötter, M.; Dehne, H. *J. Chem. Phys.* **1998**, *108*, 9062.
(24) Hiramatsu, N.; Hirakawa, S. *Polymer* **1980**, *12*, 105.

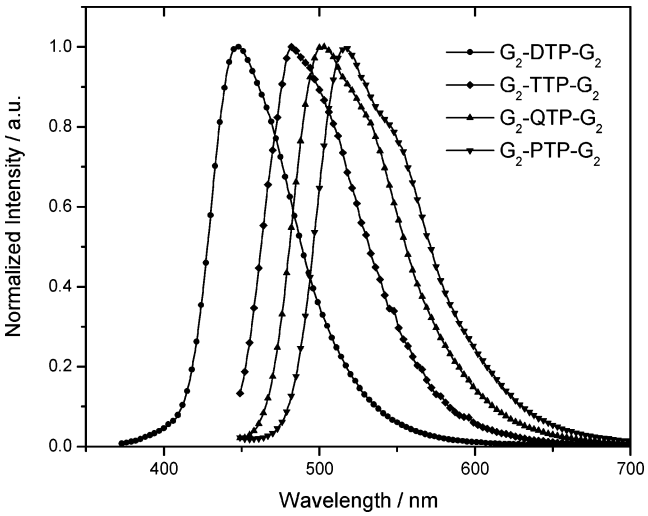

Figure 3. Fluorescence spectra of G_2-OTP(n)-G_2 in chloroform excited at 436 nm except G_2-DTP-G_2 excited at 360 nm.

Table 1. Physical Properties of G_2-OTP(n)-G_2

	absorption band,[a] nm	λ^{em}_{max},[a] nm	Φ_{360}[a,d]	ETE,[a,e] %	Φ_{436}[a,g]	T_g,[h] °C	T_{dec},[i] °C
G_2-DTP-G_2	342	448[b]	0.32	f	f	167	563
G_2-TTP-G_2	332/390	482[c]	0.11	82	0.07	171	575
G_2-QTP-G_2	329/416	503[c]	0.22	66	0.17	170	560
G_2-PTP-G_2	332/434	518[c]	0.43	69	0.31	172	544

[a] Measured in $CHCl_3$. [b] Excited at 360 nm. [c] Excited at 436 nm. [d] Using 9,10-diphenylanthrancene ($\phi_{313} = 0.9$) as a standard. [e] Estimated by comparing the absorption spectrum with the fluorescence excitation spectrum recorded at the λ_{em} of the oligothiophene core. [f] Unable to determine accurately due to peak overlapping. [g] Using fluorescein in 0.1 N NaOH ($\phi_{436} = 0.92$) aqueous solution as a standard. [h] Determined by differential scanning calorimeter from remelt after cooling with a heating rate of 10 °C/min under N_2. [i] Determined by thermal gravimetric analyzer with a heating rate of 10 °C/min under N_2.

As a result, the optical band gaps decrease with the lengthening of the oligothiophene cores. The emission spectra recorded are identical upon excitation either at the dendritic wedges (330 nm) or at the oligothiophene core (370−430 nm), which implies that energy or exciton can efficiently transfer from the peripheral wedges to the thiophene core. The energy transfer efficiencies (ETEs) of this dendritic wedge to the oligothiophene cores are in the range of 65−80%, which were estimated according to a literature method[25] by comparing the absorption spectrum with the fluorescence excitation spectrum recorded at the λ_{em} of the oligothiophene core. The PL efficiencies of these dendrimers were measured at room temperature in dilute $CHCl_3$ solution by comparing the PL intensity with that of a standard solution of fluorescein in 0.1 N NaOH ($\phi_{436} = 0.92$) according to a literature method.[26] In general, the PL efficiency increases with an increase in the length of the oligothiophene core. Table 1 summarizes the physical properties of dendrimers G_2-OTP(n)-G_2.

Electrochemical Study. To investigate the electrochemical properties of dendrimers G_2-OTP(n)-G_2 and estimate their HOMO and LUMO energy levels, cyclic voltammetry measurements were carried out under argon in a three-electrode cell using 0.1 M Bu_4NPF_6 in anhydrous CH_2Cl_2 as the supporting electrolyte. The Ag quasireference electrode was calibrated using a ferrocene/ferrocenium (Fc/Fc^+) redox couple (4.8 eV below the vacuum level)[27] as an external standard, and the $E_{1/2}$ of the Fc/Fc^+ redox couple was found to be 0.42 V versus the Ag quasireference electrode. Therefore, the HOMO energy levels of the dendrimer materials can be estimated using the empirical equation $E_{HOMO} = E_{1/2}^{ox} + 4.38$ eV, where $E_{1/2}^{ox}$ stands for the first half-wave oxidation potential relative to the Ag quasireference electrode. The results are summarized in Table 2.

Table 2. Electrochemical Properties and Estimated Energy Levels of G_2-OTP(n)-G_2

sample	$E_{1/2}^{ox}$,[a] V	E_{HOMO},[b] eV	E_g, eV (UV)[c]	E_{LUMO},[d] eV
G2-DTP-G2	0.68, 0.88, 1.20	5.06	2.91	2.15
G2-TTP-G2	0.78, 0.91, 1.08	5.16	2.65	2.51
G2-QTP-G2	0.66, 0.85	5.04	2.50	2.54
G2-PTP-G2	0.72, 0.93	5.10	2.37	2.73

[a] Measured in anhydrous CH_2Cl_2 under Ar using 0.1 M Bu_4NPF_6 as the supporting electrolyte. $E_{1/2}^{ox}$ stands for half-wave oxidation (p-doping) potentials versus a Ag quasireference. [b] Estimated from the first $E_{1/2}^{ox}$ + 4.38 eV. [c] Optical energy gaps calculated from the edge of the electronic absorption band. [d] Estimated from E_{HOMO} and optical E_g.

As can be seen from Figure 4, G_2-DTP-G_2 exhibits three reversible or quasireversible anodic redox couples. The first two redox pairs correspond to the sequential removal of electrons from the dendritic wedge because G_2-H has two redox couples at very similar potentials. In addition, the potentials of these two redox pairs remain more or less unchanged throughout the G_2-OTP(n)-G_2 series. The third anodic redox couple ($E_{1/2} = 1.20$ V vs Ag) of G_2-DTP-G_2 is assigned to the oxidation of the dithiophene unit. This redox couple shifts to lower potentials with increasing oligothiophene conjugation length from 2 to 5 thiophene units. Similar behavior has been frequently reported in the literature.[28,29] For instance, in this study, the oxidation potential of the terthiophene unit in G_2-TTP-G_2 is at $E_{1/2} = 1.08$ V versus Ag. Meanwhile, the redox waves, corresponding to the oxidation of the oligothiophene cores of G_2-QTP-G_2 and G_2-PTP-G_2, overlap with the anodic redox waves of the dendritic wedge. Unfortunately, no cathodic reduction waves for this series of dendrimers could be observed with CH_2Cl_2 as the solvent. However, their LUMO energy levels can be estimated from their HOMO energy and optical energy gaps.

Optimization of the PCBM Loading in the Dendrimer-Based Solar Cells. To evaluate the performance of the dendrimers G_2-OTP(n)-G_2 as light-absorbing and hole-transporting materials in PV devices and investigate the effect of the conjugation length of the oligothiophene core, bulk heterojunction solar cells were fabricated using a widely used fullerene derivative, PCBM, as an electron acceptor. Chlorobenzene was used as the solvent due to the better solubility of PCBM in chlorobenzene and the better nanocrystalline

(25) Stryer, L.; Haugland, R. P. *Proc. Natl. Acad. Sci. U.S.A.* **1967**, *58*, 719.
(26) Geng, Y. H.; Chen, A. C. A.; Ou, J. J.; Chen, S. H. *Chem. Mater.* **2003**, *15*, 4352.
(27) Pommerehe, J.; Vestweber, H.; Guss, W.; Mahrt, R. F.; Bassler, H.; Porsch, M.; Daub, J. *Adv. Mater.* **1995**, *7*, 551.
(28) Pappenfus, T. M.; Mann, K. R. *Inorg. Chem.* **2001**, *40*, 6301.
(29) Barbarella, G.; Favaretto, L.; Zambianchi, M.; Pudova, O.; Arbizzani, C.; Bongini, A.; Mastragostino, M. *Adv. Mater.* **1998**, *10*, 551.

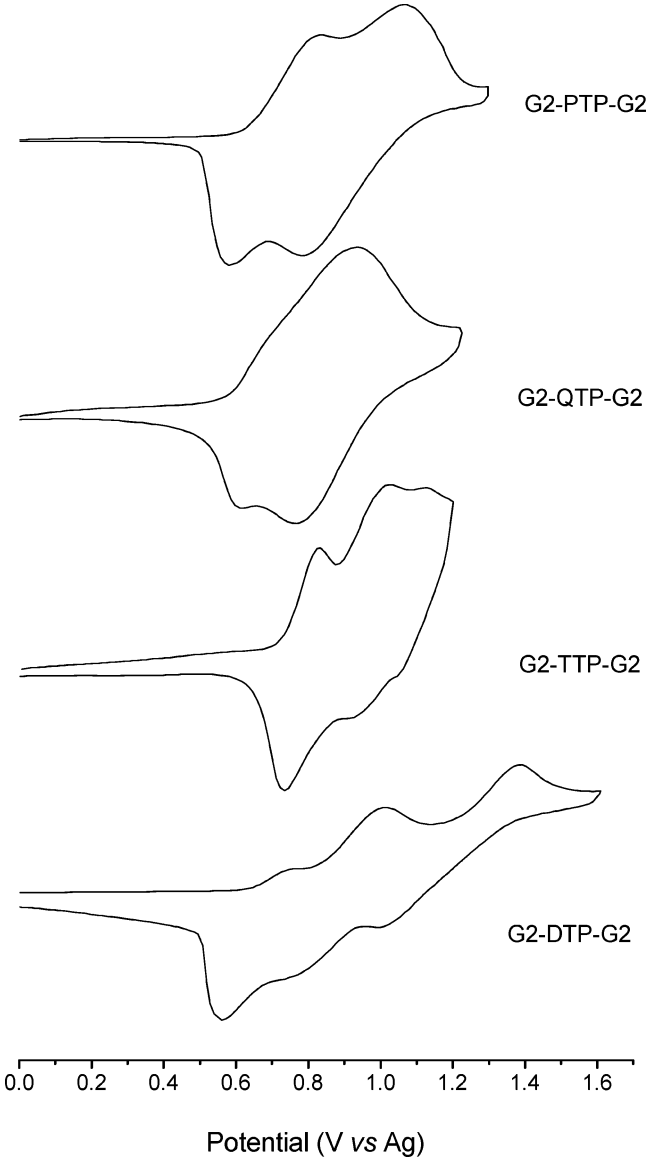

Figure 4. Cyclic voltammograms of G_2-OTP(n)-G_2 in anhydrous CH_2Cl_2.

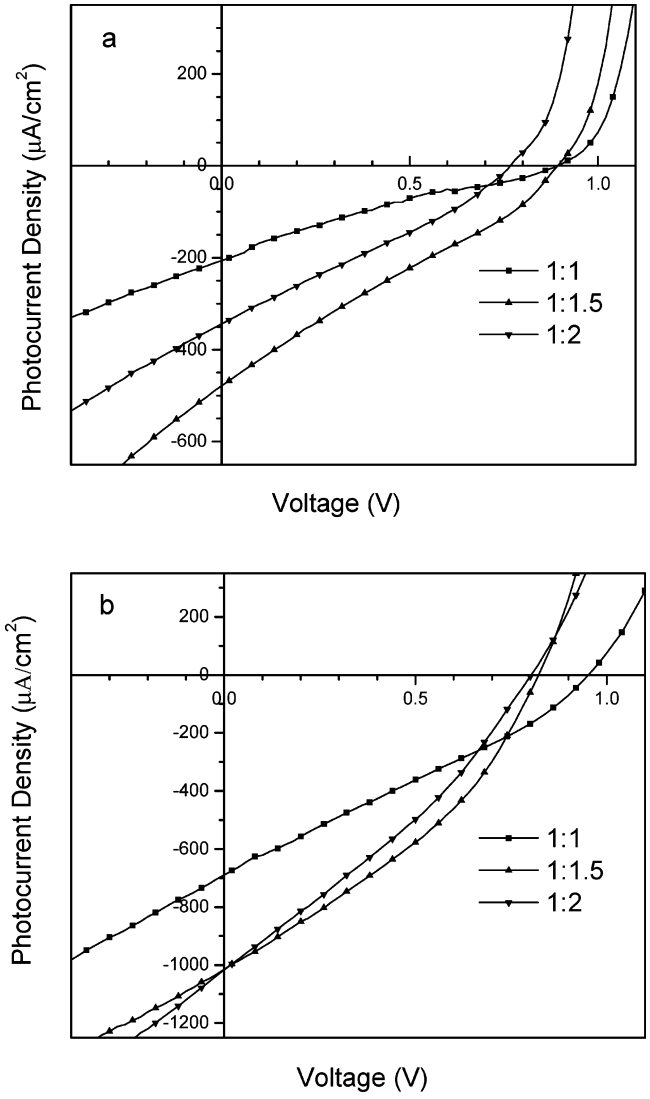

Figure 5. $J-V$ characteristics (AM 1.5, 100 mW/cm^2) of the G_2-TTP-G_2/PCBM based solar cells at different weight ratios: (a) as-fabricated devices and (b) annealed at 150 °C for 15 min under nitrogen.

packing of the active components in the resulting film.[30] It is well-known that the open-circuit voltage (V_{oc}) of an organic bulk heterojunction solar cell is primarily determined by the energy difference between the HOMO of the electron donor and the LUMO of electron acceptor. However, the dependence of the V_{oc}, J_{sc} (short-circuit current density), and FF (fill factor) on the fullerene content has been reported.[31,32]

To achieve optimum device performance, the G_2-TTP-G_2/PCBM pair was studied, and their weight ratios were varied from 1:1 to 1:1.5 to 1:2. In the mean time, the solution's total solid content was also adjusted accordingly in order to obtain a constant film thickness for the active layer in each device at a given spin rate. As can be seen from Figure 5, the best device performance was achieved at the G_2-TTP-G_2/PCBM weight ratio of 1:1.5 for both as-fabricated and annealed devices. At this ratio, the devices had the lowest series resistance (~30 Ω cm^2) and highest shunt resistance (~ 7 MΩ cm^2). It was found that the open-circuit voltage decreased with increasing PCBM content. This was probably due to the increased contact between the PEDOT electrode and the PCBM phase at higher loadings.[8,32] We also found that short-time annealing at 150 °C under nitrogen significantly improved device performance for all three PCBM contents, leading to higher short-circuit currents and greater fill factors. These improvements were attributed to the burning of shunts and increasing ordering in the active layer after thermal annealing.[7] The PV performance parameters are tabulated in Table 3. A more detailed investigation of $J-V$ characteristic curves revealed that the device shunt resistances, derived from the slope of the dark $J-V$ curves close to 0 V, increased by an order of magnitude upon annealing at 150 °C for 15 min. However, the series resistances were not reduced after annealing. This is in contrast to the polythiophene/PCBM system, which usually shows a significant decrease in series resistance after annealing.[9,10] This discrepancy can be explained by the fact

(30) Rispens, M. T.; Meetsma, A.; Rittberger, R.; Brabec, C. J.; Sariciftci, N. S.; Hummelen, J. C. *Chem. Commun.* **2003**, 2118.
(31) Campos, L. M.; Tontcheva, A.; Gunes, S.; Sonmez, G.; Neugebauer, H.; Sariciftci, N. S.; Wudl, F. *Chem. Mater.* **2005**, *17*, 4031.
(32) Van Duren, K. J.; Yang, X.; Loos, J.; Bulle-Lieuwma, C. W. T.; Sieval, A. B.; Hummelen, J. C.; Janssen, R. A. J. *Adv. Funct. Mater.* **2004**, *14*, 425.

Table 3. Effects of the PCBM Content on PV Device Performance

G_2-TTP-G_2/PCBM	V_{oc},[a] V	J_{sc},[a] μA/cm^2	FF[a]	PCE,[a] %
1:1	0.90 [b]	203[b]	0.21[b]	0.038[b]
	0.95 [c]	690[c]	0.28[c]	0.18[c]
1:1.5	0.89 [b]	477[b]	0.26[b]	0.11[b]
	0.82 [c]	1011[c]	0.35[c]	0.29[c]
1:2	0.77 [b]	342[b]	0.28[b]	0.074[b]
	0.80 [c]	1017[c]	0.31[c]	0.25[c]

[a] Under AM 1.5 simulated solar illumination at an irradiation intensity of 100 mW/cm^2. [b] For as-fabricated devices. [c] For annealed devices.

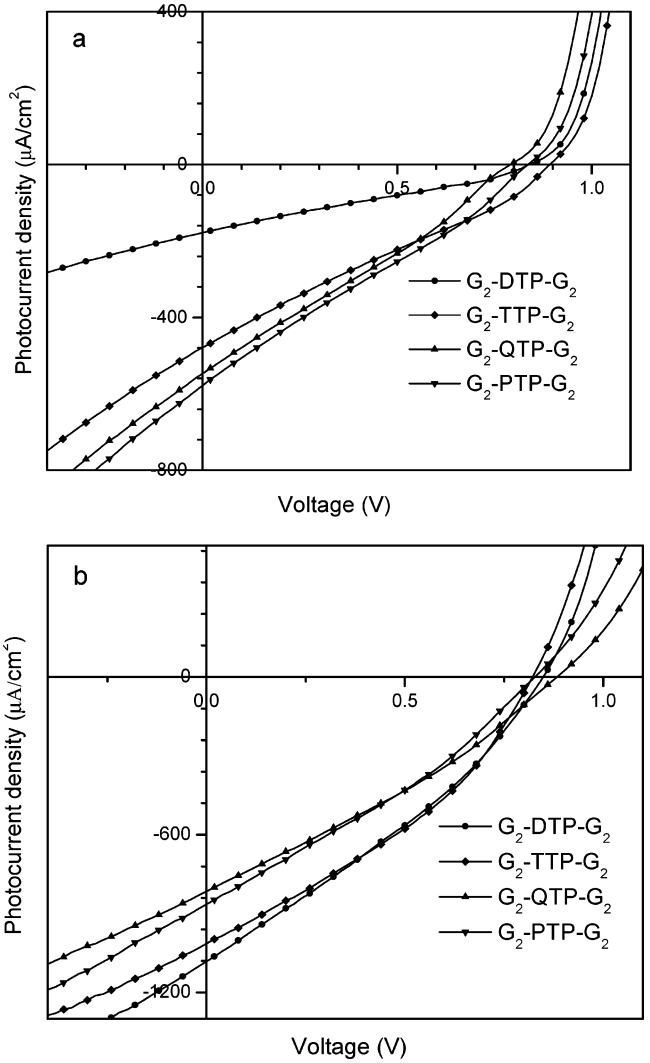

Figure 6. $J-V$ characteristics (AM 1.5, 100 mW/cm^2) of the 1/1.5 G_2-OTP(n)-G_2/PCBM based solar cells: (a) as-fabricated devices and (b) annealed at 150 °C for 15 min under nitrogen.

that regioregular poly(3-alkylthiophene)s are highly crystalline polymers while G_2-TTP-G_2 is an amorphous material.

Comparison of G_2-OTP(n)-G_2 as Electron-Donor Materials for Heterojunction Solar Cells. To systematically investigate the effect of the oligothiophene core on the PV device performance, a series of bulk heterojunction solar cells using the blend films of G_2-OTP(n)-G_2 and PCBM (1:1.5 by weight) as an active layer were fabricated. Figure 6 displays the PV response of these devices under the AM 1.5 simulated solar illumination at an irradiation intensity of 100 mW/cm^2. As can be seen from Figure 6, the device performance, such as J_{sc} and PCE, is enhanced with increasing the length of the oligothiophene core. This is in good agreement with the increased optical absorption of the active layers, as shown in Figure 7. However, after annealing at 150 °C for 15 min under nitrogen, the devices based on G_2-DTP-G_2 and G_2-TTP-G_2 showed the greatest improvement. Especially for G_2-DTP-G_2 based devices, the short-circuit current density was increased by 5 times. This dramatic improvement in device performance cannot be attributed to the increase in the optical absorption because UV−vis absorption measurements showed negligible change in the absorption spectra before and after thermal annealing for all G_2-OTP(n)-G_2/PCBM based devices. We also attempted to measure the fluorescence quantum efficiencies of the blend films using an integrating sphere. It was found that even before annealing no fluorescence from G_2-OTP(n)-G_2 was detectable. This suggests that the excitons of G_2-OTP(n)-G_2 were completely quenched by PCBM at the PCBM loading level used in this study. Considering the very limited changes in the absorption spectra, the enhanced photocurrent generation after the annealing is most likely caused by the improved charge carrier mobility and/or charge separation, instead of by improved light harvesting.[8] Since G_2-DTP-G_2 is a crystalline material, thermal annealing at 150 °C may generate semicrystalline structures, as confirmed by DSC analysis. This may explain the good performance of G_2-DTP-G_2 in annealed solar cells with $J_{sc} = 1082$ μA/cm^2, $V_{oc} = 0.85$ V, FF $= 0.31$, even though it has the lowest absorption in the visible region among this series of dendrimers. Although X-ray diffraction (XRD) is a standard method for the investigation of crystalline structures, our preliminary XRD study on the G_2-DTP-G_2/PCBM film did not show crystalline peaks. This result is not surprising, considering that G_2-DTP-G_2 is not prone to crystallize and PCBM and G_2-DTP-G interfere with each other in the formation of crystalline structures. However, AFM measurements did show the increase in the maximum surface roughness from 2.67 to 4.69 nm and formation of some aggregates after thermal annealing, as shown in Figure 8, indicating the presence of some ordered nanocrystalline structures. The PV performance data for the G_2-OTP(n)-G_2/PCBM based devices are summarized in Table 4. We also

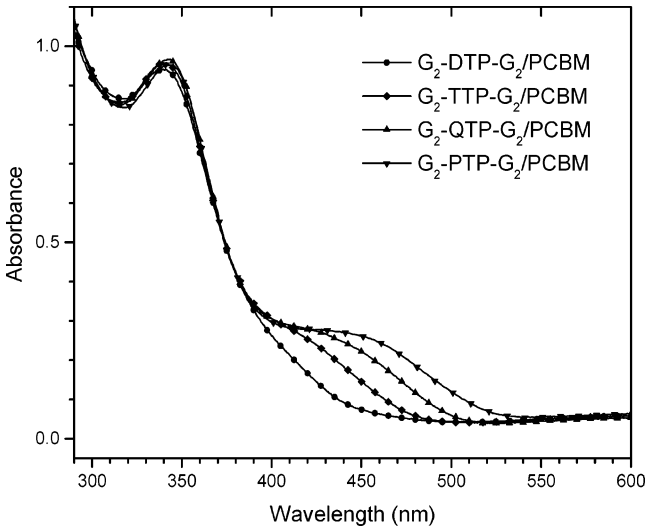

Figure 7. UV−vis absorption spectra of the blend films of G_2-OTP(n)-G_2 and PCBM (1:1.5 by weight).

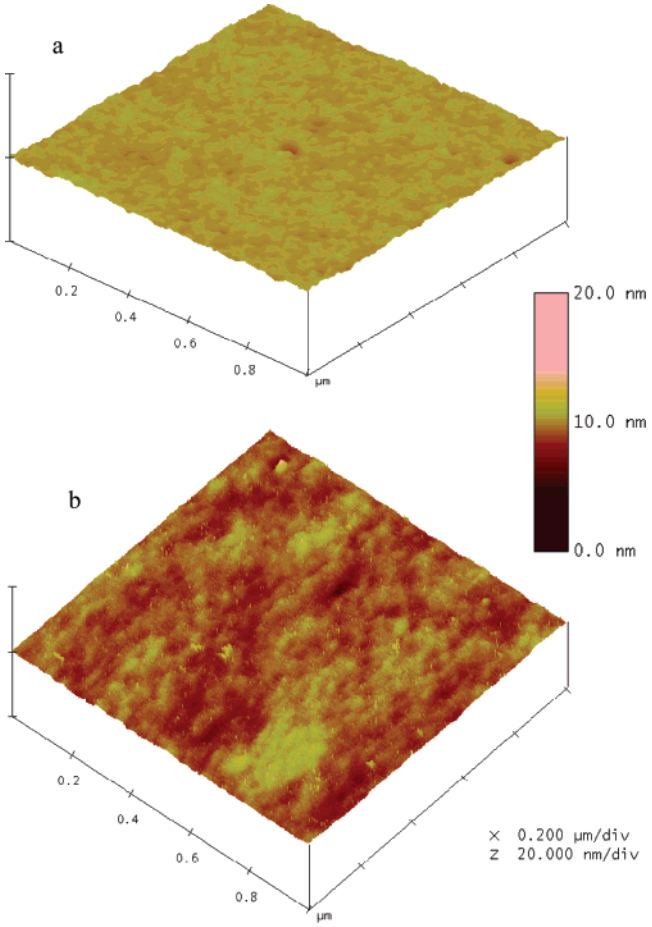

Figure 8. AFM images of the G_2-DTP-G_2/PCBM blend films (a) before and (b) after thermal annealing.

Table 4. Summary of Device Performance for 1/1.5 G_2-OTP(n)-G_2/PCBM Based PV Devices

electron donors	V_{oc},[a] V	J_{sc},[a] μA/cm^2	FF[a]	PCE,[a] %
G_2-DTP-G_2	0.84[b]	177[b]	0.27[b]	0.04[b]
	0.85[c]	1082[c]	0.31[c]	0.28[c]
G_2-TTP-G_2	0.89[b]	477[b]	0.26[b]	0.11[b]
	0.82[c]	1011[c]	0.35[c]	0.29[c]
G_2-QTP-G_2	0.79[b]	547[b]	0.27[b]	0.12[b]
	0.88[c]	814[c]	0.30[c]	0.22[c]
G_2-PTP-G_2	0.84[b]	578[b]	0.28[b]	0.13[b]
	0.83[c]	864[c]	0.30[c]	0.22[c]

[a] Under simulated AM 1.5 solar illumination at an irradiation intensity of 100 mW/cm^2. [b] For as-fabricated devices. [c] For annealed devices.

attempted to increase annealing temperature to 165 °C, which is close to the T_g's of the dendrimers. However, the thermal treatment at this temperature resulted in device breakdown due to the pronounced change in the film morphology, which was visible even by naked eyes.

Electroluminescent Properties of G_2-DTP-G_2 and G_2-PTP-G_2. As G_2-DTP-G_2 and G_2-PTP-G_2 showed reasonable fluorescence quantum efficiencies in $CHCl_3$ solution, these two compounds were tested as hole transport emitters in OLEDs with a configuration of ITO/PEDOT-PSS/G_2-OTP(n)-G_2/TPBI/LiF/Al. TPBI was used as a hole-blocking layer to increase electron−hole recombination efficiency in the emitting layer. Usually the solid-state FL efficiencies of polythiophenes and oligothiophenes are low due to the increased contribution of nonradiative decay via interchain

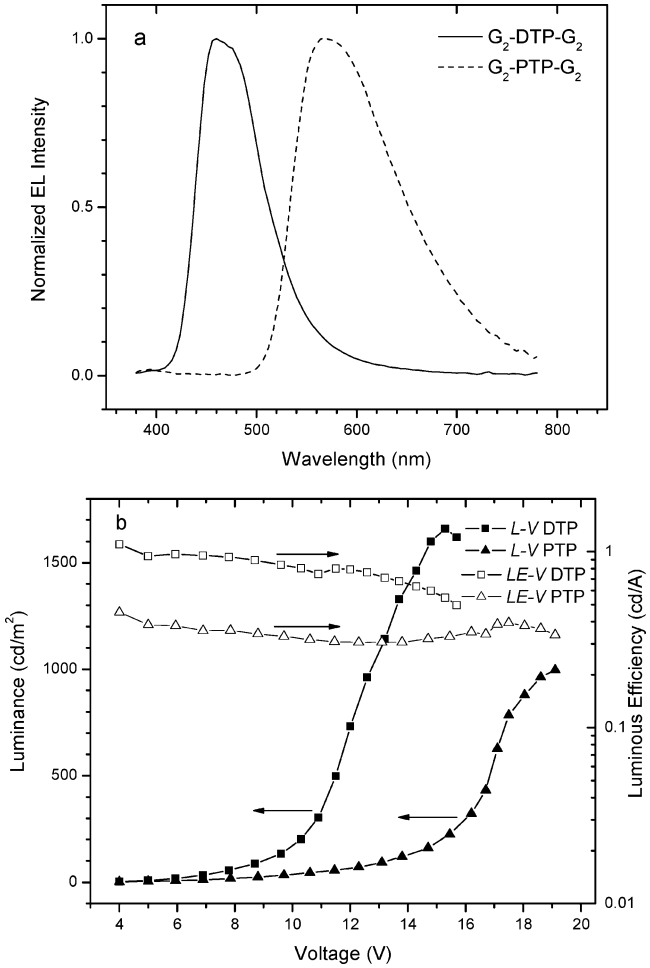

Figure 9. (a) EL spectra and (b) $L-V$ characteristics of G_2-DTP-G_2 and G_2-PTP-G_2 based devices.

interactions and intersystem crossing caused by the heavy-atom effect of sulfur.[19,20] G_2-DTP-G_2 (0.18) and G_2-PTP-G_2 (0.07) have a moderate solid-state FL efficiency because of the presence of the dendritic wedges at the end of the oligothiophenes, which can prevent the oligothiophene cores from strongly interacting with each other. It is worth pointing out that G_2-DTP-G_2 has a higher thin-film FL efficiency than G_2-PTP-G_2 although its solution FL efficiency is lower.

Since both G_2-DTP-G_2 and G_2-PTP-G_2 have a high HOMO energy level, the energy barrier for the hole injection from PEDOT−PSS to the emissive layer is almost negligible. As a result, the turn-on voltages for both devices, corresponding to 1 cd/m^2, were as low as 4 V. The EL spectra and $L-V$ characteristics of the fabricated devices are shown in Figure 9. G_2-DTP-G_2 exhibited blue electroluminescence with CIE 1931 coordinates (0.160, 0.191), while G_2-PTP-G_2 emitted yellow light with CIE coordinates (0.499, 0.493). The CIE coordinates of both devices remained unchanged until the devices were burned. The maximum luminance of G_2-DTP-G_2 based devices reached 1660 cd/m^2 at 15.5 V, and the luminous efficiency was above 0.75 cd/A over a luminance range from 20 to 1000 cd/m^2. On the contrary, the maximum luminance of G_2-PTP-G_2 based devices only reached 1000 cd/m^2 at 19 V, and the luminous efficiency was as low as 0.35 cd/A at 300 cd/m^2. If we took the photopic response into account, the G_2-DTP-G_2 based devices are far superior

to the G_2-PTP-G_2 based devices. The stronger intermolecular interaction and thus lower solid-state FL efficiency of G_2-PTP-G_2 may account for its poorer performance in OLEDs.

Conclusions

In this study, we report on the synthesis and functional property investigation of a novel series of multi-triarylamine-substituted carbazole-based dendrimers G_2-OTP(n)-G_2 bearing an oligothiophene as a functional core. It was found that both the absorption and photoluminescence (PL) emission peaks red-shifted with increasing oligothiophene core length, leading to a better match for the solar spectrum. However, their HOMO energy levels remain almost unchanged because the HOMO energy, in this case, is primarily determined by the first oxidation potential of the dendritic wedge, rather than by the oligothiophene core. Bulk heterojunction solar cells using the G_2-OTP(n)-G_2/PCBM blend films as an active layer were fabricated. The PCBM loading level was optimized. The as-fabricated devices showed enhanced performance with increasing oligothiophene conjugation length. This is in agreement with the increase in the optical absorption of the active layers. However, after thermal annealing at 150 °C for 15 min, the G_2-DTP-G_2 devices showed the most dramatic improvement due to the formation of some ordered structures in the active layer. Although the overall power conversion efficiencies obtained in this study are not high (∼0.3%) because of the low absorption in the solar spectrum, the insight gained here will provide some hints for the development of new light-absorbing hole transport materials, such as optimal band gaps (approaching 1.5 eV), high crystallinity, and high charge mobility. In addition, we have demonstrated that G_2-DTP-G_2 was able to function as hole-transporting blue emitters in OLEDs with a low turn-on voltage of 4 V, a maximum luminance of 1660 cd/m^2 at 15.5 V, and at 130 cd/m^2.

Acknowledgment. We are grateful to the Hong Kong Research Grants Council (HKBU 2018/05P) for financial support of this work. We also thank Simona Moisa and Guy Parent at IMS for the AFM measurements and Dr. Jianfu Ding at ICPET, NRC, for the GPC analysis.

Supporting Information Available: ^{1}H NMR spectra and GPC profiles of multi-triarylamine-substituted carbazole-based dendrimers G_2-OTP(n)-G_2 ($n = 2-5$). This material is available free of charge via the Internet at http://pubs.acs.org.

CM062111O